PAPER Nr. : 7

INFLUENCE OF FUSELAGE ON ROTOR INFLOW PERFORMANCE AND TRIM

By

A. DEHONDT

Ecole Nationale Supérieure
de Mécanique et d'Aérotechnique
Poitiers, FRANCE

F. TOULMAY

Aérospatiale S.N.I.
Division Hélicoptères
Marignane, FRANCE

AEROSPATIALE HELICOPTER DIVISION
MARIGNANE, FRANCE

FIFTEENTH EUROPEAN ROTORCRAFT FORUM

SEPTEMBER 12 - 15, 1989 AMSTERDAM

INFLUENCE OF FUSELAGE ON ROTOR INFLOW PERFORMANCE AND TRIM

Arnaud DEHONDT
Ecole Nationale Supérieure
de Mécanique et d'Aérotechnique
Poitiers, FRANCE

François TOULMAY
Aérospatiale S.N.I.
Division Hélicoptères
Marignane, FRANCE

ABSTRACT

The correlation between a new rotor code and extensive velocity measurements performed at NASA Langley Research Center is showing that the interference from the fuselage significantly modifies the inflow in the front part of the rotor disk; in the rear part, the inviscid flow prediction of the fuselage effect fails presumably due to the wake of the rotor hub and upper cowlings. A crude but satisfactory approximation of the actual inflow is obtained, in this case, by computing with the fuselage perturbation velocity on the front half disk and without it on the rear half disk.

Under the influence of the fuselage and for constant rotor forces, the induced power is sharply reduced and this explains a similar but lower reduction in total power. The cyclic pitch required to trim the rotor laterally is augmented under the influence of the fuselage. The magnitude of these effects is highly dependent on the actual downwash in the rear half disk.

INTRODUCTION

Several research studies have already demonstrated the extent of the fuselage's influence on the main rotor's performance and vibration (ref. 1-2-3). These studies are mainly based on theoretical analyses of the velocities induced by the fuselage as well as the deformations generated in the blades' wake.

In the absence of local velocity measurements however, the validity of this approach can only be estimated with blades' dynamic load measurements i.e. a very indirect confirmation compromised by many other inaccuracies (airfoil aerodynamics, blade dynamic modelization). This naturally limits the degree of confidence granted to these analyses.

The recent publication of velocities measured with laser velocimetry by NASA Langley (ref. 5) gives an opportunity to directly check not only the isolated rotor's calculation codes (ref. 7) but also the improvements offered by the interaction models (ref. 8). The METAR code which was previously correlated to airload data only (experimental helicopters SA349GV and Puma, ref. 12) is now being extended to compare the time-averaged inflow in a survey plane above the rotor and takes the fuselage induced perturbations into account. It is hoped that this will help better understand model deficiencies and determine the fields where every approximation level is acceptable.

The rotor/fuselage performance problem will be reviewed with enhanced confidence in the analysis tools once this milestone has been passed.

EXPERIMENT

An experimental investigation was conducted in the 4.3 x 6.7 meter wind tunnel at NASA Langley Research Center to measure the rotor inflow of a model helicopter in forward flight (ref. 5, 6, 4). Two velocity components were measured 76 mm above the tip path plane with a laser velocimeter. Only the time averaged component normal to the tip path plane is considered in the present correlation.

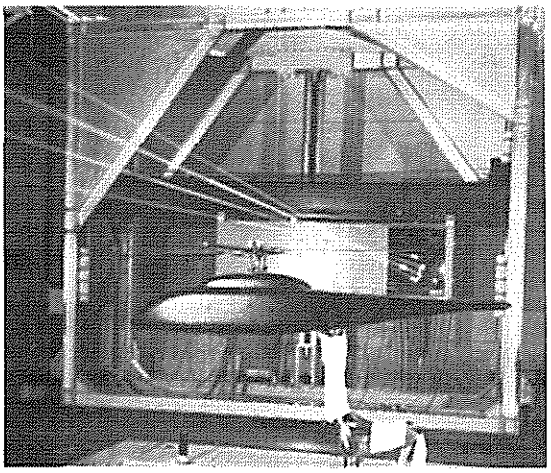

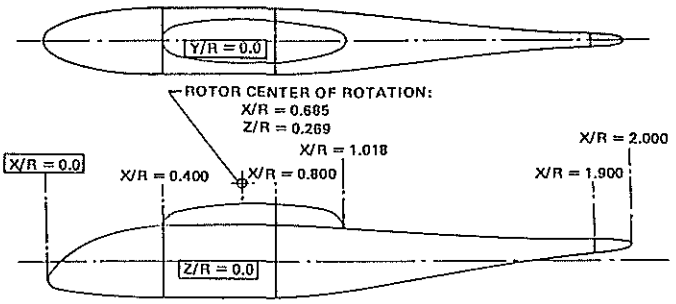

Figure 1 : Model fuselage

(Courtesy of U.S. Army Aerostructures Directorate at the NASA Langley Research Center)

TABLE 1: CHARACTERISTICS OF RECTANGULAR BLADES			
HUB TYPE	articulated	NUMBER OF BLADES	4
AIRFOIL	NACA0012	LINEAR TWIST	-8 deg
RADIUS	0.8606 m	CHORD	0.066 m
HINGE OFFSET	0.0508 m	ROOT CUTOUT	0.2096 m
BLADE MASS	0.259 Kg	RADIUS OF C.G.	0.330 m

Two sets of blades have been tested, but only one is considered in the present study. These blades feature a classical rectangular planform (cf. Table 1). Three flight conditions i.e. μ = 0.15 - 0.23 - 0.30 are reported in reference 5. Table 2 recalls the test conditions for the lowest and highest advance ratios only. Calculations have also been performed for the μ = 0.23 case but the conclusions appeared to be intermediate between the other two, making it less interesting and it is not therefore reported here.

TABLE 2 : TEST CONDITIONS		
ADVANCE RATIO	0.30	0.15
SHAFT ANGLE (°)	-4.04	-3.00
TIP MACH NUMBER	0.5364	0.5533
THRUST Ct	0.00649	0.0063
CONING ANGLE (°)	2.13	1.50
FLAP ANGLES (°)	0./0.	0./0.

The shape of the fuselage (fig. 1) is a hybrid design that is representative of configurations in common use throughout the world, but not a model of any specific helicopter. The contours are defined by simple algebraic formulae (ref. 6).

CALCULATION MODEL

Isolated rotor

The rotor is aerodynamically modelized with the METAR code developed by Aérospatiale where the blades are considered as lifting lines localized at the forward quarter chord. The continuous distribution of circulation along the span is discretized with a step function. Smaller steps are clustered near the tip since most important aerodynamic phenomena are known to occur in this region (fig. 2).

The vortex layer leaving the trailing edge is replaced with a lattice of linear vortex segments which intensity is related to the variation in circulation span and azimuth wise (fig. 3). Once the marginal vortex has rolled up (Betz theory), this lattice is reduced to a tip and root vortex forming the far wake. Wake geometry can be prescribed with empirical formulae inspired from Egolf and Landgrebe work (ref. 9) or with the conventional cycloidal trajectories which are generally sufficient for high speed conditions.

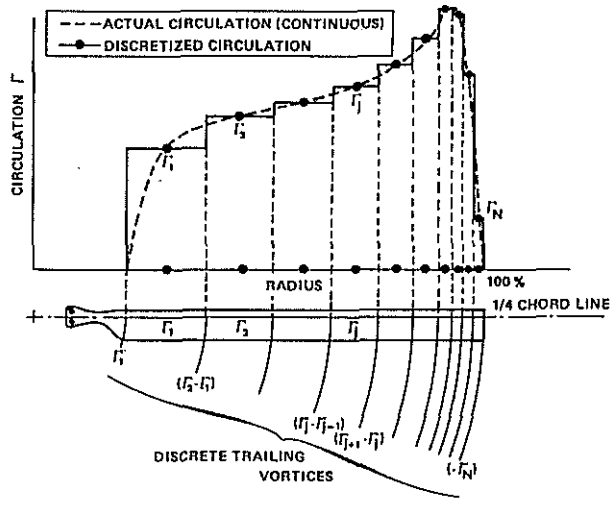

Figure 2 : Spanwise discretization of circulation

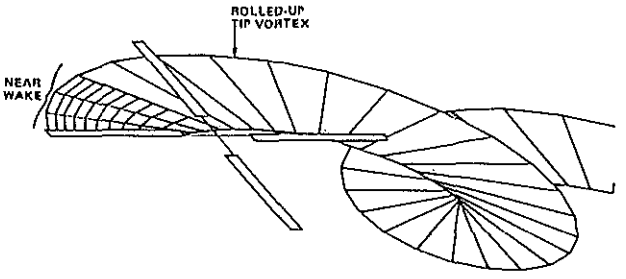

Figure 3 : Rotor wake discretization

Starting from a known blades/wake position, the influence matrices determining the velocity induced at control points are calculated as a function of the circulation at those points (Biot and Savart law).

A second set of equations linking induced velocity and circulation is needed to solve the problem. It is obtained in the classical manner assuming a steady two dimensional flow about the airfoil. Lift is derived from the calculation of incidence and Mach number with the experimental airfoil tables. The Joukowski relation $L = \rho V \Gamma$ then helps determine circulation Γ.

Blades motion is calculated simultaneously by coupling with the blade dynamics code R85 also developed by Aérospatiale. Blades are, in this study, considered rigid and hinged in flap only. This aerodynamics/dynamics problem is solved iteratively with a relaxation method where induced velocities are the unknowns (fig. 4).

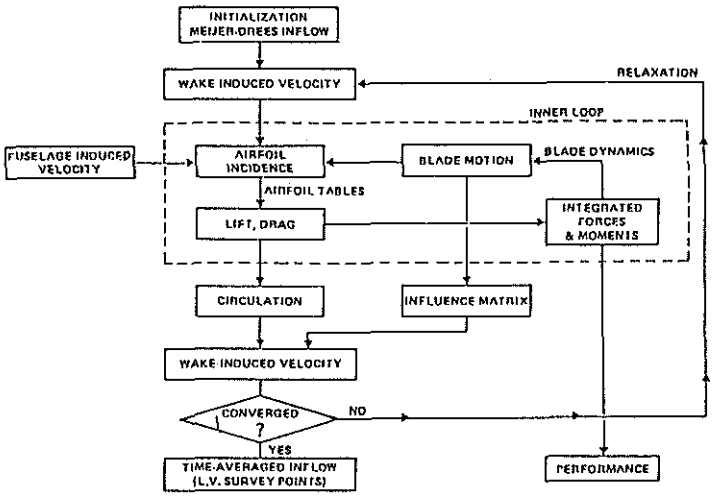

Figure 4 : Flow chart of rotor analysis

Isolated fuselage

Code WBAERO provided by A.M.I. uses quadrangular panels with a constant density of source type singularities. 700 panels approx were used for the NASA model (fig. 5). Symmetry helped discretize only half of the fuselage. For some calculations, the mechanical parts composing the rotor hub were also represented with an axisymmetrical body of equivalent volume.

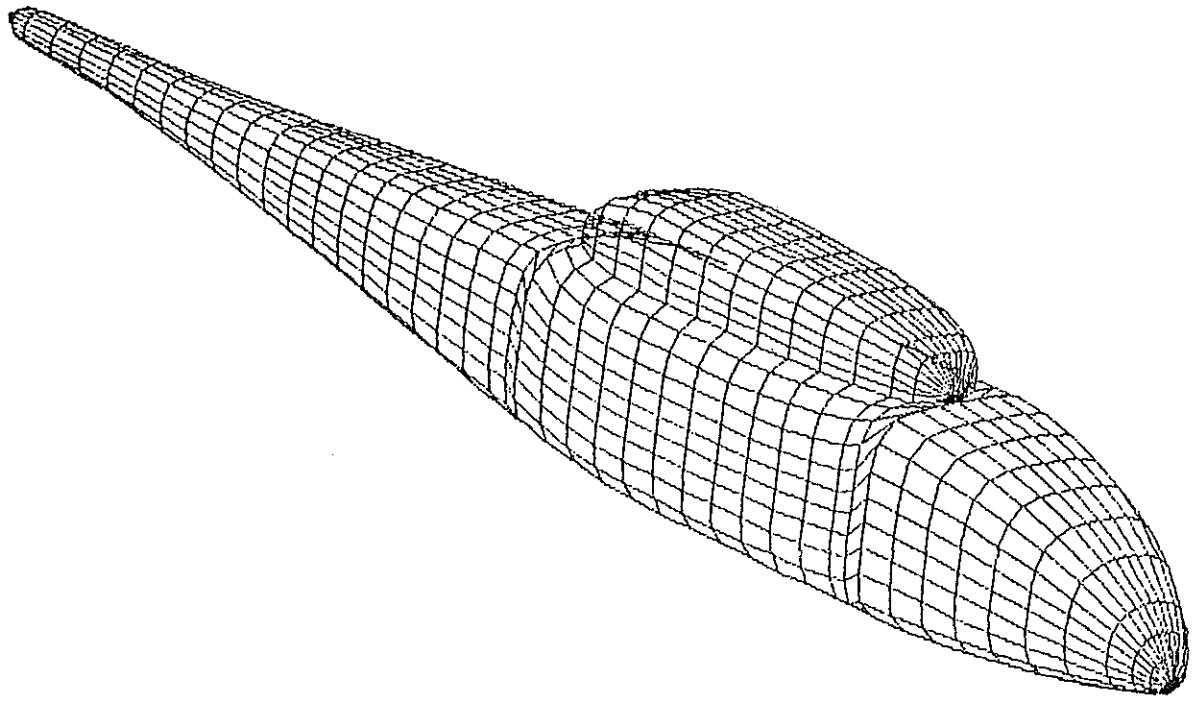

Figure 5 : Panel discretization of the fuselage

Incidence varied very little in the speed envelope explored i.e. - 1° for μ = 0.3 to 0° for μ = 0.15. As recommended by Wilby & al. (ref. 1), only one fuselage calculation was undertaken at zero incidence. A same calculation can naturally be used whatever the upstream velocity may be because of the linearity of the equations. Velocities expressed in a non dimensional manner Vx/Vo, Vy/Vo and Vz/Vo were calculated at blade control points as well as survey points above the rotor.

Fuselage-influenced rotor

The velocity vectors calculated by WBAERO are expressed in airfoil coordinates at every blade control station, and only the component normal to the chordline is retained in computing the local angle of attack. This approximation is consistent with the calculation of wake induced velocity which also retains the normal component only. The wake geometry is unchanged with respect to an isolated rotor calculation, but the intensity of shed and trailed vortices is being modified as a result of a different distribution of circulation on the blade. The fuselage effect consists therefore of two parts :

- a direct contribution from the fuselage-induced inflow,
- a indirect contribution through modified wake-induced inflow.

The inflow calculated at survey points is time averaged over a quarter revolution for comparison with time averaged test data.

COMPARISON OF CALCULATED AND MEASURED INFLOWS

Rotor inflow due to fuselage influence

The contour plot of Figure 6 presents the vertical component of velocity in the rotor tip path plane, as computed by WBAERO (isolated fuselage). The rotor is represented as seen from the top, rotating counterclockwise, with the blade in aft position (ψ = 0°) on the right hand side.

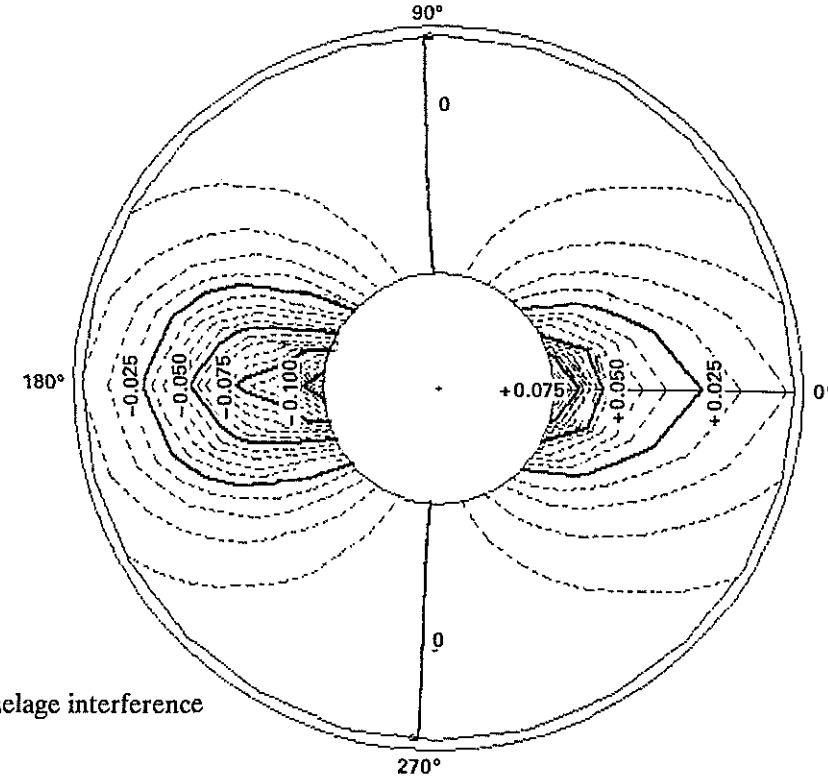

Figure 6 : Rotor inflow due to fuselage interference

The inflow pattern appears not only symmetrical about the longitudinal axis - this results from the no sideslip asumption - but also nearly antisymmetrical front to aft, with the zero inflow line running diametrically from one side to the other. Due to the fuselage's slender shape and the rotor's position, the upwash above the canopy is only slightly larger than the downwash above the tail cone. The advancing and retreating sides of the disk remain unaffected by the fuselage.

Control law

Two calculations have been performed for each configuration, one for the isolated rotor and the other for the fuselage perturbated rotor. Both results have been compared to the experiment. In order to draw meaningful conclusions from this comparison and, particularly for performance, it is necessary to trim the rotor at the same thrust and propulsive force. The thrust is adjusted to the experimental value (Table 2) with the collective pitch as the control parameter.

The propulsive force, which is not directly documented in NASA reports, is a function of the tip path plane position which was controlled during test : the flap angles β_{1c} and β_{1s} were trimmed to zero with the cyclic controls θ_{1s} and θ_{1c}. The same procedure is used in the calculation. It has been checked that the propulsive force is not affected by the fuselage inflow.

The flap moment of inertia which is not documented has been calculated from the known CG position assuming a constant mass distribution along the span : Ib = 0.05 Kg.m^2 (Lock number $\simeq$ 5). This value gives a coning angle which does not depart from the measured coning by more than 0.2 deg.

For the low speed flight case i.e. μ = 0.15, the calculation is taking into account the distorted wake geometry. This effect is important at low speed only. The wake is, in these conditions, slowly convected away from the blades. In the intermediate case i.e. μ = 0.23, the difference with the classical undistorted wake is hardly noticeable and can be neglected for the high speed case i.e. μ = 0.30.

Results at $\mu = 0.30$

This case where the free stream velocity is higher is expected to demonstrate the higher influence of the fuselage upon the rotor inflow. This influence can be assessed by different complementary representations i.e. comparison of contour plots (Fig. 7), radial (Fig. 9a) and azimuthal (Fig. 9b) distribution of inflow.

As already observed by Hoad & al. (ref. 7) the portion of the rotor disk with a negative (velocity upwards) inflow is underestimated in the isolated rotor calculation (Fig. 7b). The calculation with fuselage influence (Fig. 7c) shows a clear improvement, with the zero-inflow line retreating up to the blade root and the apparition of a saddle shaped contour similar to that of the experiment about azimuth $\psi = 180°$.

From Fig. 9b, it can be seen that the peak-to-peak amplitude of inflow versus azimuth is somewhat underestimated in the calculation, with the error being concentrated on the front part of the disk in the $\psi = 90°$ to $270°$ range. However, the inflow induced by the fuselage is improving the shape of the curves about $\psi = 180°$ in a very significant manner.

The radial distribution of inflow (Fig. 9a) is reporting very little fuselage influence on the advancing and retreating sides ($\psi = 90°$ and $270°$) as was anticipated in Figure 6. The shape of the calculated curves is matching the data points quite well, except for a constant offset of about 1.5 m/s. This offset is just another aspect of the error previously noted on the azimuthal distribution. It can also be observed with several other computer codes that have been correlated with the same data (ref. 7 and 8).

In the front part ($\psi = 180°$), fuselage simulation is dramatically improving the correlation. The hub is only affecting the inflow in close proximity, up to 30% radius, with better results in this limited region.

In the rear part ($\psi = 0°$), the effect of the fuselage is also high, but clearly deteriorating. This trend is even more visible on the azimuthal distribution (Fig. 9b) at 40% radius where the best correlation is obtained with fuselage influence for $\psi = 90°$ to $270°$ and without fuselage influence for $\psi = 270°$ to $360°$, and $0°$ to $90°$.

A tentative explanation is offered on Fig. 11. The pressure gradient is favorable in the front part of the fuselage, and the boundary layer remains thin and attached to the body. The upwash predicted by the potential flow code is therefore a fair approximation of the real flow in this region.

But some separation might be present on the tail's upper part due partly to the blunt end of the upper cowlings and also to the hub wake combining with the general adverse pressure gradient. The descending flow pattern, typical of the inviscid solution, is then replaced in the real flow by an eddy wake which does not deflect the streamlines located in the rotor plane above.

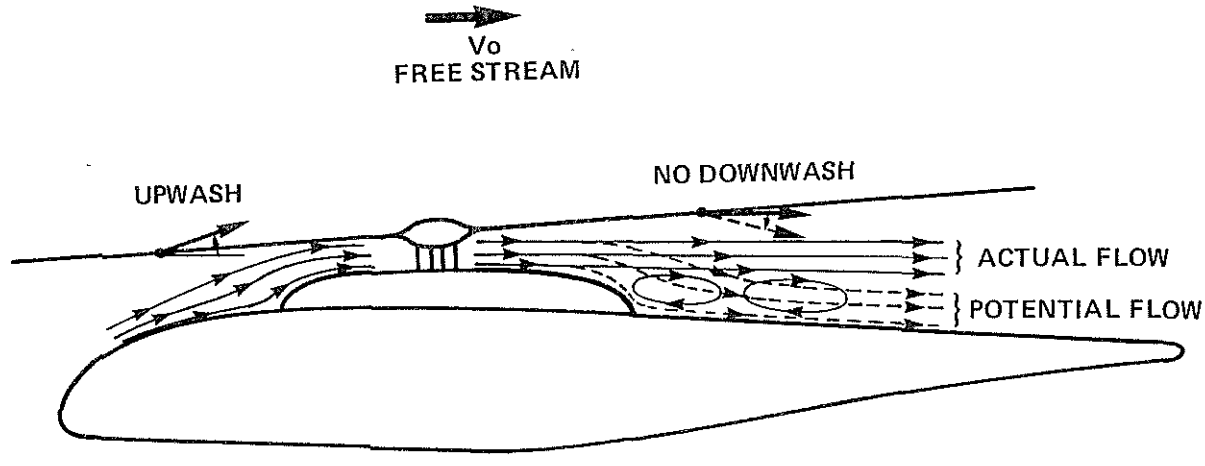

Figure 11 : Influence of fuselage wake on rotor inflow

This could explain why the rotor calculations without the fuselage downwash are better in the rear part of the disk. The inflow distribution at 78% and 98% radius (Fig. 9b) are confirming the importance of fuselage effect about azimuth $\psi = 180°$ and the absence of downwash about $\psi = 0°$.

Figure 7:

Inflow contour plots

- μ = 0.30

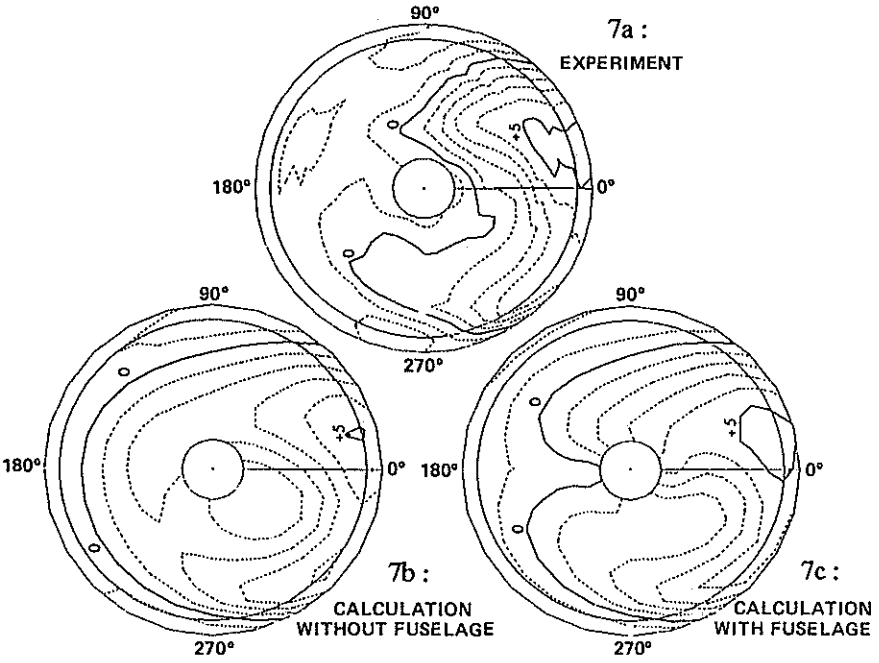

Figure 9a :

Inflow radial distribution

- μ = 0.30

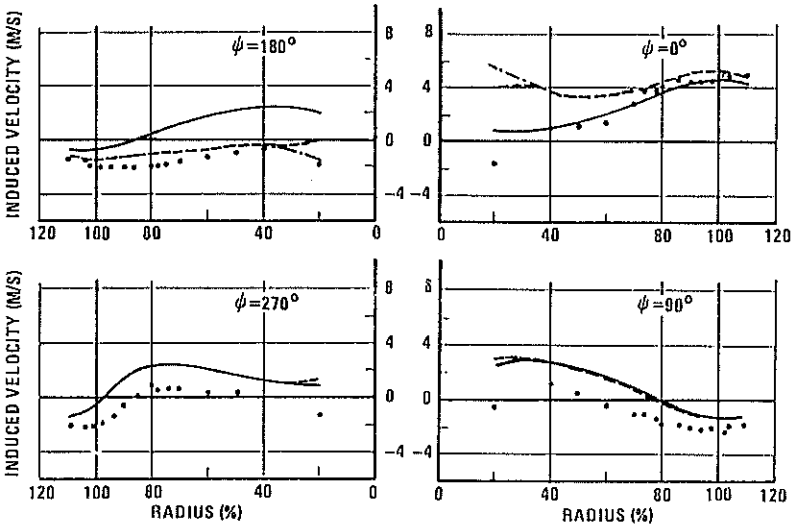

• L.V. DATA
——CALCULATION WITHOUT FUSELAGE
– – –CALCULATION WITH FUSELAGE
—·—CALCULATION WITH FUSELAGE & HUB

Figure 9b :

Inflow azimuthal distribution

- μ = 0.30

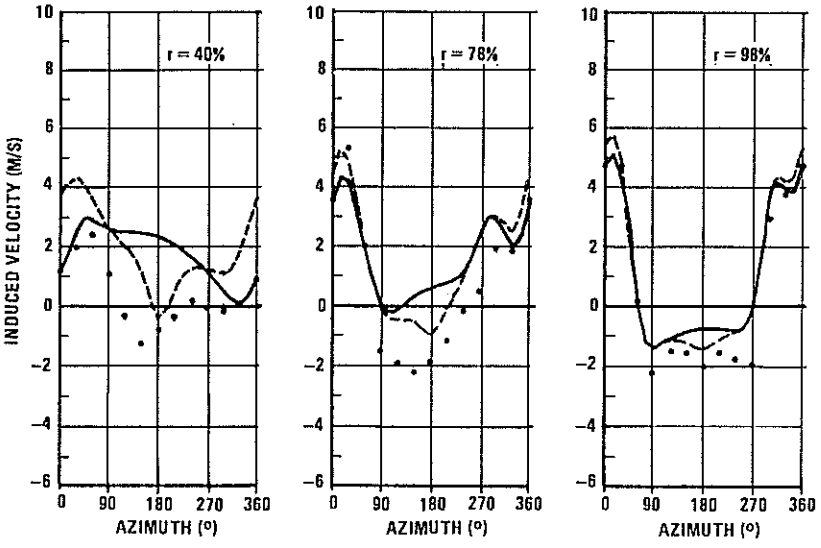

Fig b: μ= 0,30 –

Results at $\mu = 0.15$

The correlation between calculations and test data (see Fig. 8 and 10) is again satisfactory in general, but not ideal in detail.

The contour plots and the azimuthal distribution of inflow are confirming that the peak-to-peak variation of inflow is underestimated, with errors being now more concentrated on the rear part. The steep slope observed on the advancing side at 78% radius is not properly matched by the calculations. This is even more apparent on Fig. 10a at $\psi = 90°$ azimuth.

The computed effect of the fuselage is naturally much less in this low speed case. It is however still beneficial in the front part (fig. 8). At $\psi = 0°$ (Fig. 10a), the shape of the curve is deteriorated despite the fact that it is compensating the error locally near the hub. It would therefore appear again that the downwash calculated by inviscid codes should not be applied on the rear part of the disk.

The comparison of calculated inflow and experimental data for both high and low speed has proven the general validity of the rotor analysis, despite the underestimated fore-to-aft asymmetry and local gradient at $\psi = 90°$ and 270°. The comparison has also indicated the need to include corrections for the fuselage influence in the front part of the disk. These corrections are deteriorating the correlation in the rear part of the disk, presumably because of flow separation behind the hub and cowlings.

PERFORMANCE AND TRIM

The effect of fuselage interaction on rotor performance and trim parameters will now be investigated. The experimental set-up did not permit isolated rotor configurations, and these investigations can only then be based on the computational model.

Simulated conditions

A velocity sweep from $\mu = 0.15$ to 0.42 has been performed with four inflow options :

1. Meijer-Drees' inflow, isolated rotor, with a 10% correction for tip loss
2. METAR inflow, isolated rotor
3. METAR inflow, with fuselage interference (WBAERO)
4. METAR inflow, with fuselage interference corrected for wake i.e. no downwash on the rear half disk.

The Meijer-Drees' model (ref. 10), a refined version of Froude/Glauert's momentum theory, can be classified as a uniform inflow model. It compares very poorly with measured inflow patterns but offers the advantage of a simple formulation and is currently frequently used as a reference for simulation and performance estimates.

Comparisons are conducted in conditions similar to those of the high speed experimental case ($\mu = 0.30$) :

$$U_{tip} = 190 \text{ m/s} \quad C_t = 0.0065 \quad \alpha_{shaft} = -4° \quad \beta_{ls} = 0$$

In order to simulate level flight at various speeds, the propulsive force is ajusted in such a way as to balance drag with an equivalent flat plate area $D/q = 0.20 \text{ m}^2$. This value has been selected to exactly match the test at $\mu = 0.30$ so that the longitudinal flap β_{lc} cancels out at this speed.

The calculated flap angle β_{lc} and the propulsive force will obviously not match the experiment at advance ratio $\mu = 0.15$ or 0.23 and this precludes any valid comparison in terms of power or pitch. No meaningful conclusion can be drawn from a single test point at $\mu = 0.30$. There were thus no attempt to correlate the calculated trim or performance and the data.

Figure 8 :

Inflow contour plots

- μ = 0.15

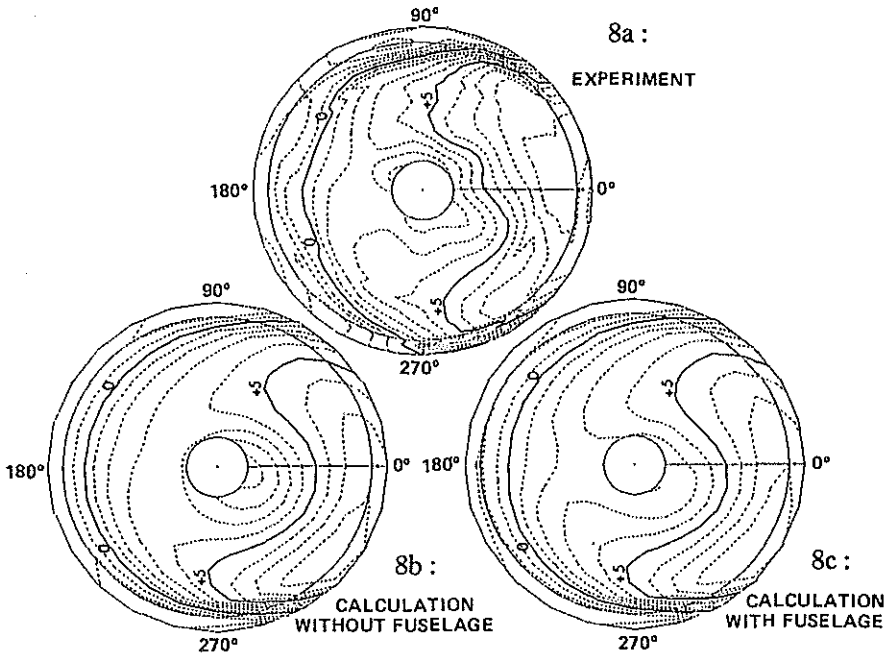

Figure 10a :

Inflow radial distribution

- μ = 0.15

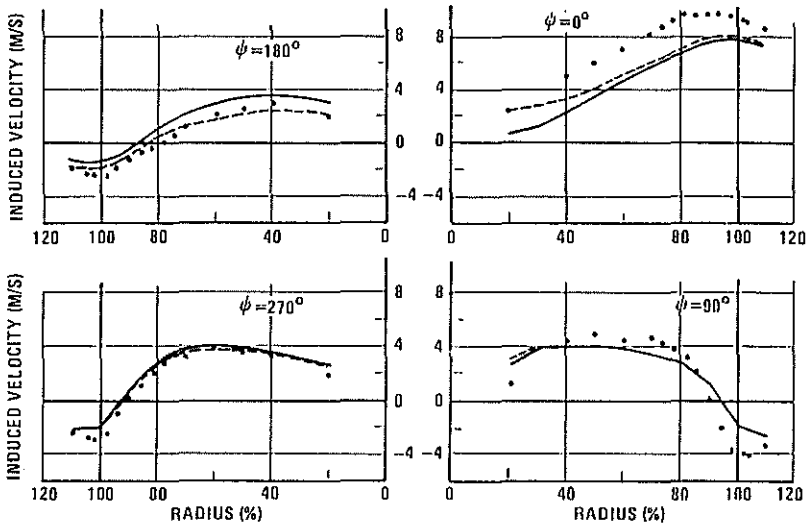

• L.V. DATA
——CALCULATION WITHOUT FUSELAGE
– – –CALCULATION WITH FUSELAGE
—·—CALCULATION WITH FUSELAGE & HUB

Figure 10b :

Inflow azimuthal distribution

- μ = 0.15

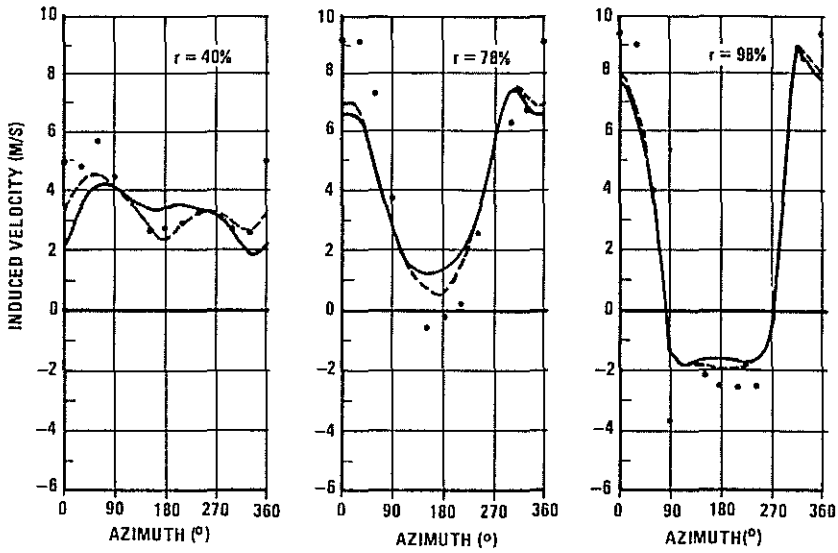

Fig b: μ= 0,15 –

Induced power (Fig. 12)

The Meijer-Drees' model results in a decreasing induced power with increasing advance ratio, as is usual with uniform inflow theory. The power is somewhat higher in the other three calculations, because of a the highly non-uniform inflow (Fig. 7). The difference between uniform and non uniform inflow is larger at low speed because of radial non uniformity, and at high speed also because of negative inflow in the front part of the rotor. Ripples on the curves are occurring because of variations in the pattern of blade/vortex interactions as the advance ratio is being changed.

The fuselage induced inflow, when not corrected for wake, does not very much modify the performance i.e. the positive inflow on the rear half disk (downwash) is increasing power nearly as much as the negative inflow is decreasing it in the front half. When the downwash is suppressed to simulate the wake however, the effect of the fuselage is becoming quite large i.e. -18% of the induced power at $\mu = 0.36$.

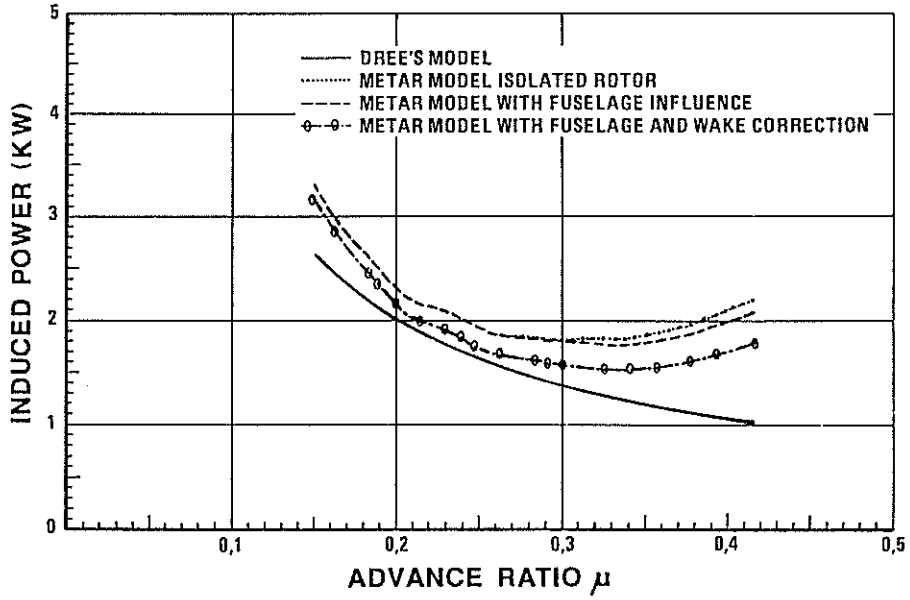

Figure 12 : Calculated influence of fuselage on induced power

Total rotor power (Fig. 13)

Although some changes in airfoil drag occur with inflow redistribution as a consequence of fuselage perturbations, the previous conclusions also hold for total power. The effect of fuselage upon power is comprised between -3% and 0 depending on the advance ratio and whether the wake correction is used or not.

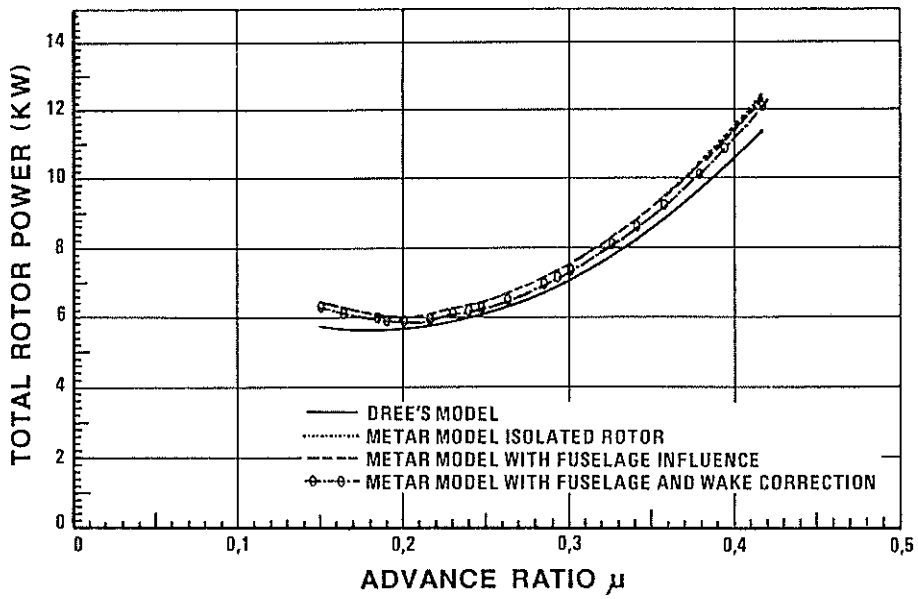

Figure 13 : Calculated influence of fuselage on total rotor power

It should be noted that the calculation with Drees' model remains quite close to that with METAR inflow, fuselage and wake corrections for advance ratios ranging from 0.2 to 0.35. This range coincides with the cruise speed of present helicopters against which Drees' model has been validated and found satisfactory for performance prediction.

Lateral cyclic pitch (Fig. 14)

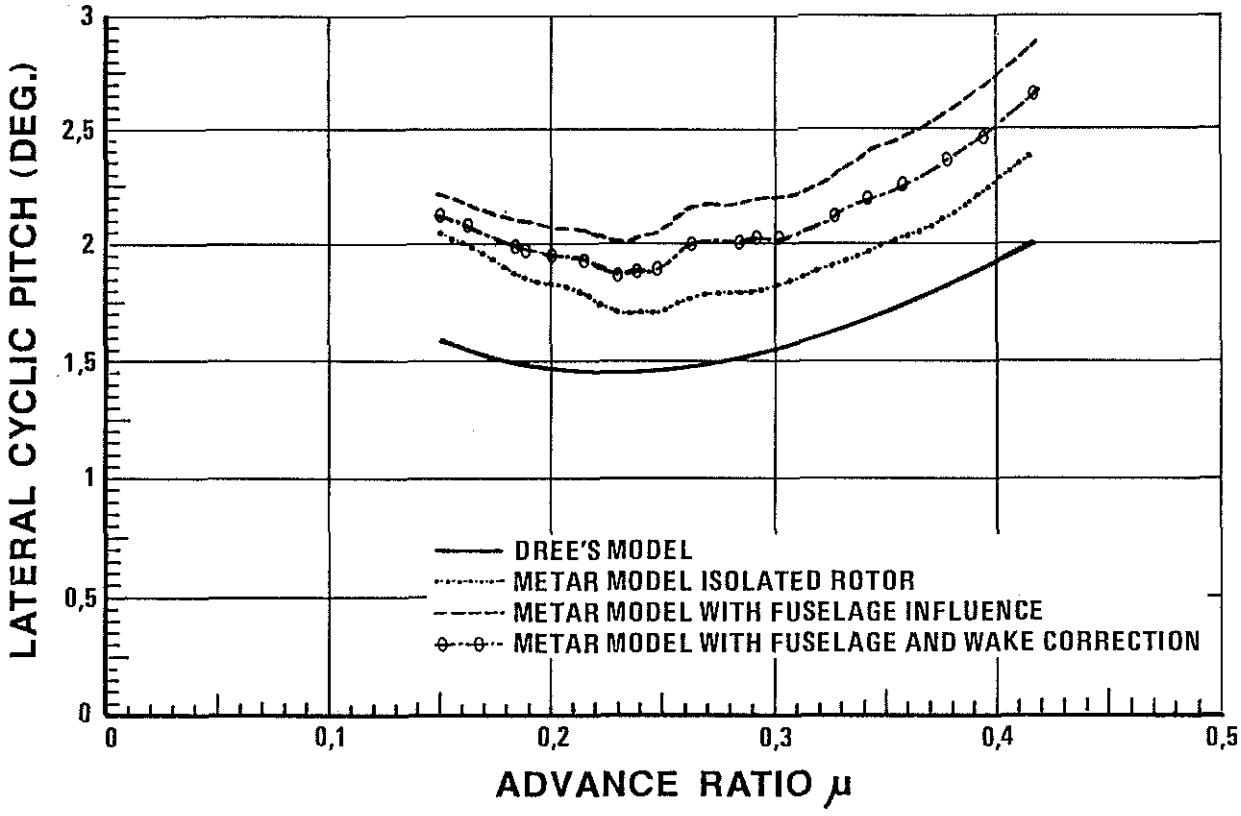

Figure 14 : Calculated influence of fuselage on lateral cyclic pitch

The rotor coning makes the application of some lateral cyclic pitch necessary to ensure blade equilibrium in forward flight. The Meijer-Drees' formulation includes a linear variation of inflow along the longitudinal axis which also plays a role in the required cyclic pitch (Fig. 14). This front-to-aft inflow gradient, as calculated with METAR, is higher and therefore calls for even more cyclic pitch. The inflow due to fuselage influence is still increasing the gradient and, consequently, increasing the required cyclic pitch again.

Cancelling downwash on the rear half disk reduces the gradient change by roughly a factor of two, it is thus no surprise to find this curve half way between the isolated and the fuselage influenced rotor. Again, the ripples can be traced to the changing blade/vortex interactions pattern.

Assuming the wake correction to be correct, the effect of the fuselage on cyclic pitch would amount to about 0.25 deg.

The effect on other parameters i.e. collective pitch, longitudinal cyclic, longitudinal rotor tilt, or lateral force has been found negligible.

CONCLUSIONS

The extensive rotor inflow survey performed at the NASA Langley Research Center makes it possible to assess the validity of a rotor wake analysis in a direct manner. Although the tests were not intentionally dedicated to studying fuselage/rotor interference, the results do show velocity perturbations which are undoubtedly associated to the fuselage body.

This study can hardly be considered as complete. Potentially important points such as rotor wake distortions, rotor-to-fuselage interference, fuselage wake modelling, or vibrations have not been addressed. Only one rotorcraft configuration has been analysed while the effects are sensitive to the fuselage shape and rotor/fuselage relative position, as mentioned in previous works (ref. 1-2-3-4). Some definite conclusions are however emerging which should be useful guidelines for further developments :

- The fair correlation of METAR results with test data is proving the basic soundness of the code for inflow calculation (confirmed by airload analysis in other applications, ref. 12).
- Some deficiencies, also apparent in other analyses of the same data (ref. 7 and 8) are observed on the advancing and retreating sides where the high inflow gradients remain underpredicted.
- An appreciable improvement of the velocity pattern is obtained over the front half of the rotor when fuselage-induced inflow perturbations are included in the analysis.
- A potential flow analysis of the fuselage is found inadequate for modelling the velocity on the rear half of the rotor plane, because of flow separation behind the hub and cowlings. Better correlations are observed when the calculated downwash is arbitrarily set to zero.
- The fuselage influence is reducing the total rotor power by as much as 3% for the NASA fuselage at advance ratio $\mu = 0.30$.
- The lateral cyclic pitch is slightly augmented by 0.25 deg approx by the effect of the fuselage.

The fuselage global effects on the rotor appears to be highly dependent on the extent of recirculation and eddy wake behind the hub and cowlings. Therefore, any further attempt to modelize the interference should analyse this phenomenon more extensively. This calls for appropriate experimental data.

ACKNOWLEDGEMENTS

The authors wish to thank MM. Wayne Mantay and Danny Hoad of the U.S. Army Aerostructures Directorate at the NASA Langley Research Center for providing informations regarding the experiment.

REFERENCES

1) P.G. WILBY, C. YOUNG and J. GRANT, "An Investigation of the Influence of Fuselage Flow Field on Rotor Loads, and the Effects of Vehicule Configuration", 4th European Rotorcraft Forum, Stresa, 1978

2) H. HUBER and G. POLZ, "Studies on Blade-to-Blade and Rotor-Fuselage-Tail Interferences", AGARD CP 334, London, 1982

3) W. JOHNSON and G.K. YAMAUCHI, "Applications of an Analysis of Axisymmetric Body Effects on Rotor Performance and Loads", 10th European Rotorcraft Forum, The Hague, 1984

4) C.E. FREEMAN and J.C. WILSON, "Rotor-Body Interference (ROBIN) - Analysis and Test", 36th Annual Forum of the American Helicopter Society Washington D.C., 1980

5) J.W. ELLIOTT, S.L. ALTHOFF and R.H. SAILEY, "Inflow Measurement Made with a Laser Velocimeter on a Helicopter Model in Forward Flight", Volumes I, II, III, NASA Technical Memoranda 100541 to 100543 (1988)

6) A.E. PHELPS III and J.D. BERRY, "Description of the U.S. Army Small-Scale 2-Meter Rotor Test System", NASA Technical Memorandum 87762 (1987)

7) D.R. HOAD, S.L. ALTHOFF and J.W. ELLIOTT, "Rotor Inflow Variability with Advance Ratio", 44th Annual Forum of the American Helicopter Society, Washington D.C., 1988

8) D.A. PETERS and CHENG JIAN HE, "Comparison of Measured Induced Velocities with Results from a Closed-Form Finite State Wake Model in Forward Flight", 45th Annual Forum of the American Helicopter Society Boston, 1989

9) T.A. EGOLF and A.J. LANDGREBE, "Helicopter Rotor Wake Geometry and its Influence in Forward Flight", Volumes I & II, NASA Contractor Report 3727, October 1983

10) I.J. MEIJER-DREES, "A Theory of Airflow Through Rotors and its Application to Some Helicopter Problems", Journal of the Helicopter (Great Britain, 1949)

11) P.F. SHERIDAN and R.P. SMITH, "Interactional Aerodynamics - A New Challenge to Helicopter Technology", 35th Annual Forum of the American Helicopter Society, Washington D.C., 1979

12) W.G. BOUSMAN, W. JOHNSON, C. YOUNG, M.J. RILEY, F. TOULMAY, N. GILBERT "Correlation of PUMA Airloads - Lifting Line and Wake Calculation", 15th European Rotorcraft Forum, Amsterdam, 1989